Depletion of the Ras Association Domain Family 1, Isoform A–Associated Novel Microtubule-Associated Protein, C19ORF5/MAP1S, Causes Mitotic Abnormalities

Ashraf Dallol,[1] Wendy N. Cooper,[1] Fahd Al-Mulla,[2] Angelo Agathanggelou,[1] Eamonn R. Maher,[1] and Farida Latif[1]

[1]Section of Medical and Molecular Genetics, Institute of Biomedical Research, University of Birmingham, Edgbaston, Birmingham, United Kingdom and [2]Molecular Pathology Laboratory, Department of Pathology, Kuwait University, Faculty of Medicine, Safat, Kuwait

Abstract

Ras association domain family 1, isoform A (RASSF1A) is a novel tumor suppressor gene that is found to be inactivated in more than 40 types of sporadic cancers. In addition, mouse Rassf1a knockout models have an increased frequency of spontaneous and induced tumors. The mechanisms by which RASSF1A exerts its tumor suppression activities or the pathways it can regulate are not yet fully understood. Using yeast two-hybrid system, we have previously identified C19ORF5/MAP1S as the major RASSF1A-interacting protein. C19ORF5 has two conserved microtubule-associated regions and may function to anchor RASSF1A to the centrosomes. In this study, we have analyzed the cellular functions of C19ORF5. By using small interfering RNA–mediated depletion and time-lapse video microscopy, we show that C19ORF5 knockdown causes mitotic abnormalities that consist of failure to form a stable metaphase plate, premature sister chromatid separation, lagging chromosomes, and multipolar spindles. We also show that a fraction of C19ORF5 localizes to the spindle microtubules. Additionally, we show here that C19ORF5 localizes to the microtubule-organizing centers during microtubule regrowth after nocodazole washout. Knockdown of C19ORF5 disrupts the microtubule-organizing center and results in microtubule nucleation from several sites. Whereas the localization of pericentrin is not affected, α- and γ-tubulin localization and sites of nucleation are greatly altered by C19ORF5 depletion. This may indicate that C19ORF5 plays a role in anchoring the microtubule-organizing center to the centrosomes. In addition, we show that the NH_2 terminus of C19ORF5 is essential for this process. This novel role for C19ORF5 could explain the resulting mitotic abnormalities that occur on its depletion and can potentially provide an underlying mechanism for the frequent centrosome and microtubule abnormalities detected in several cancers. [Cancer Res 2007;67(2):492–500]

Introduction

There is ever increasing evidence for the classification of Ras association domain family 1, isoform A (RASSF1A) as a tumor suppressor gene (1). In addition to being found to be epigenetically inactivated in most types of sporadic cancers (2, 3), Rassf1a knockout mice have an increased predisposition to spontaneous as well as induced tumor development (4, 5). However, the mechanism(s) by which RASSF1A can exert its growth-suppressive functions are not fully understood. RASSF1A can affect the cell cycle by inhibiting the anaphase-promoting complex/Cdc20 complex (6), association with the cyclin A modulator p120E4F (7), or by regulating cyclin D1 levels (8). RASSF1A can control apoptosis by MST (9, 10) or BAX-regulated pathways (11, 12). Furthermore, depletion of RASSF1A or deletion of Rassf1a is associated with changes in the cytoskeleton and increases phosphatidylinositol 3-kinase–dependent cellular motility (13). In fact, a main feature of RASSF1A expression has been its effect on the microtubules (14–16). We have recently identified C19ORF5 (also known as BPY2IP1 or MAP1S) as a novel RASSF1A-interacting protein in a yeast two-hybrid screen of a pretransformed human brain cDNA library where clones harboring C19ORF5 constituted the majority of the positive clones identified (14). The interaction of C19ORF5 and RASSF1A was also confirmed independently by other groups (17, 18). C19ORF5 is a ubiquitously expressed member of the MAP1A/B family of microtubule-associated proteins (19). The C19ORF5-RASSF1A interaction at the centrosome is thought to be required for the proper control of the anaphase-promoting complex/Cdc20 complex during mitosis (18). Overexpression of C19ORF5 can cause mitochondrial aggregation and genome destruction (20). Interestingly, this mechanism of cell death can explain the toxic accumulation of the mouse homologue Map8 in the Gigaxonin-null mice (21). C19ORF5, as well as its other interacting partner, LRP130, can bind nucleic acids although the function of this binding is not clear (22). Despite the existence of two conserved microtubule-binding regions in C19ORF5 (23, 24), the overexpressed protein exhibits diffused cytosolic staining patterns. C19ORF5 association with the microtubules becomes more evident when cells are treated with the microtubule-stabilizing drug paclitaxel or when C19ORF5 is coexpressed with RASSF1A (14, 25). Understanding the cellular functions of C19ORF5 will provide useful insights on how the tumor-suppressive actions of RASSF1A are exerted. Therefore, we used small interfering RNA (siRNA)–mediated knockdown of C19ORF5 in HeLa cells and HeLa cells stably expressing green fluorescent protein (GFP)–tagged histone H2B (26) to study the effect of C19ORF5 depletion on mitosis. We focused on mitosis because of the reported role of C19ORF5 in the regulation of

Note: Supplementary data for this article are available at Cancer Research Online (http://cancerres.aacrjournals.org/).

Present address for A. Agathanggelou: Chromatin and Gene Expression Group. Division of Infection and Immunity, Institute of Biomedical Research, University of Birmingham, Edgbaston, Birmingham B15 2TT, United Kingdom.

Requests for reprints: Farida Latif, Section of Medical and Molecular Genetics, Division of Reproductive and Child Health, The Institute of Biomedical Research, University of Birmingham, Edgbaston, Birmingham B15 2TT, United Kingdom. Phone: 44-121-627-2741; Fax: 44-121-627-2618; E-mail: f.latif@bham.ac.uk or Ashraf Dallol, E-mail: a.dallol@bham.ac.uk.

©2007 American Association for Cancer Research.

doi:10.1158/0008-5472.CAN-06-3604

Downloaded from cancerres.aacrjournals.org on January 21, 2021. © 2007 American Association for Cancer Research.

RASSF1A-Cdc20 interaction (6), in addition to the importance of microtubules in this process.

Materials and Methods

Plasmid construction. Full-length C19ORF5 (NM_018174) was cloned by PCR from cDNA originating from the human glioma cell line H4 (ATCC HTB-148). Full-length coding region for C19ORF5 was subsequently cloned into the pGEM-T Easy vector (Promega, Southampton, United Kingdom) and the fidelity of the sequence was verified by Big Dye sequencing. C19ORF5 was subcloned into the *Hin*dIII-*Not*I sites of the pFLAG-CMV-4 (Sigma-Aldrich, Dorset, United Kingdom), which allowed the NH_2-termial tagging of C19ORF5 with a FLAG tag, FLAG-C19ORF5. The fragment amino acids (aa) 1 to 797 was generated by digestion of FLAG-C19ORF5 with *Bam*HI and religating the larger fragment. The fragment amino acids 797 to 1,059 was generated by cloning the shorter *Bam*HI fragment generated from above into pcDNA3.1-HA. HA-338-1059aa was generated by PCR cloning.

Cell lines and RNA interference. HeLa and HeLa-H2B-GFP (26) cell lines were kept in DMEM, 10% FCS, L-glutamine-penicillin-streptomycin solutions and were routinely maintained at 37°C and 5% CO_2. The double-stranded siRNA oligonucleotides targeting C19ORF5 were purchased from Ambion [Huntingdon, United Kingdom; Silencer predesigned siRNA-1 (ID 26322) and siRNA-2 (ID 45347)]. Transfection was done using the Oligofectamine reagent (Invitrogen, Paisley, United Kingdom) according to the manufacturer's recommended protocol for HeLa cells. Plasmid transfections were achieved using Lipofectamine 2000 (Invitrogen).

Antibodies, immunofluorescence, and immunoblotting. The mouse monoclonal antibody (mAb) against C19ORF5 (mAb4G1, 1:5,000 for Western blotting and 1:400 for immunofluorescence) was purchased from A&G Pharmaceuticals (Columbia, MD; ref. 20). Mouse mAbs against α-tubulin (DM1A), FLAG (M2 and M5), hemagglutinin (HA), and rabbit polyclonal anti–γ-tubulin were from Sigma-Aldrich. Rabbit polyclonal anti-HA antibody was from Santa Cruz Biotechnology (Y-11; Santa Cruz, CA). Rabbit polyclonal antibodies to pericentrin and α-tubulin were from Abcam (Cambridge, United Kingdom). Human anticentromere antibody was purchased from Antibodies, Inc. (Davis, CA); mouse anti–cyclin B1 and anti–cyclin A mAbs were obtained from the Cancer Research UK research antibodies service. Horseradish peroxidase (HRP)–conjugated rabbit anti-mouse immunoglobulin G (IgG) and HRP-conjugated goat anti-rabbit IgG secondary antibodies were purchased from DakoCytomation (Ely, United Kingdom). Alexa Fluor 594–conjugated rabbit anti-mouse IgG and Alexa Fluor 488–conjugated anti-rabbit IgG, as well as Alexa Fluor 488–conjugated anti-human IgG, were purchased from Molecular Probes (Paisley, United Kingdom).

Immunofluorescence. Staining of endogenous proteins was done on mitotic cells collected by shake-off before plating them on poly-L-lysine–coated coverslips. The cells were then preextracted with 0.2% Triton X-100 in 5% FCS in PHEM buffer (60 mmol/L PIPES, 25 mmol/L HEPES, 10 mmol/L EGTA, 2 mmol/L $MgCl_2$) for 2 min before fixation with methanol at −20°C for 10 min, followed by incubation with primary antibodies for 1 h at room temperature. The coverslips were washed extensively with PBS/0.01% Triton X-100 before incubation with the secondary antibodies for 45 min and washing. The coverslips were then mounted with VECTASHIELD containing 4′,6-diamidino-2-phenylindole (DAPI; Vector Labs, Peterborough, United Kingdom). Images were visualized with a Photometrics SenSys KAF 1400-G2 charged coupled device fitted to a Zeiss Axioplan fluorescence microscope and captured using the SmartCapture

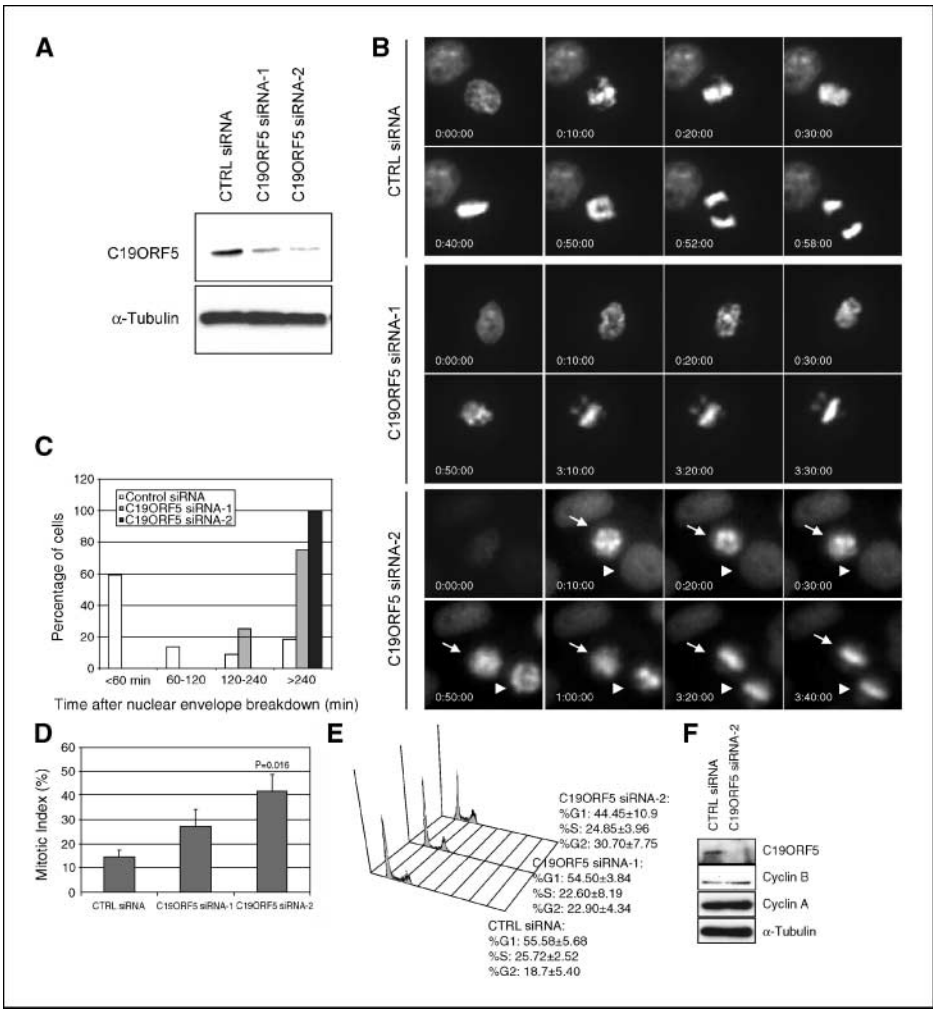

Figure 1. Knockdown of C19ORF5 delays mitosis. *A,* Western blot analysis of C19ORF5 levels after 48-h transfection of HeLa-H2B-GFP cells with control (*CTRL*) siRNA or two siRNA oligos directed against C19ORF5. α-Tubulin was used as a loading control. *B,* representative images of HeLa-H2B-GFP cells undergoing mitosis after transfection with control or C19ORF5 siRNA oligos. Time 0:00:00 is defined as the time that nuclear envelope breakdown and chromatin condensation were evident. *Arrows* and *arrowheads,* different mitotic cells. *C,* mitotic cells from different treatments were analyzed for the time between nuclear envelope breakdown and anaphase (n = 30). *Columns,* percentage of cells that divided within the time frame shown in the *X*-axis. *D,* the mitotic index was determined by counting the percentage of rounded cells to total cells (n = 500) 48 h posttransfection with the siRNA oligos indicated. *Bars,* SD of three experiments. The *P* value is determined with Student's *t* test comparing C19ORF5 siRNA-2 to control siRNA. *E,* DNA histograms showing the cell cycle fractions after treatment with the indicated oligos. Analysis was done using WinMDI and Cylchred software. *F,* detection of cyclin B and cyclin A levels after C19ORF5 depletion in HeLa cells.

Downloaded from cancerres.aacrjournals.org on January 21, 2021. © 2007 American Association for Cancer Research.

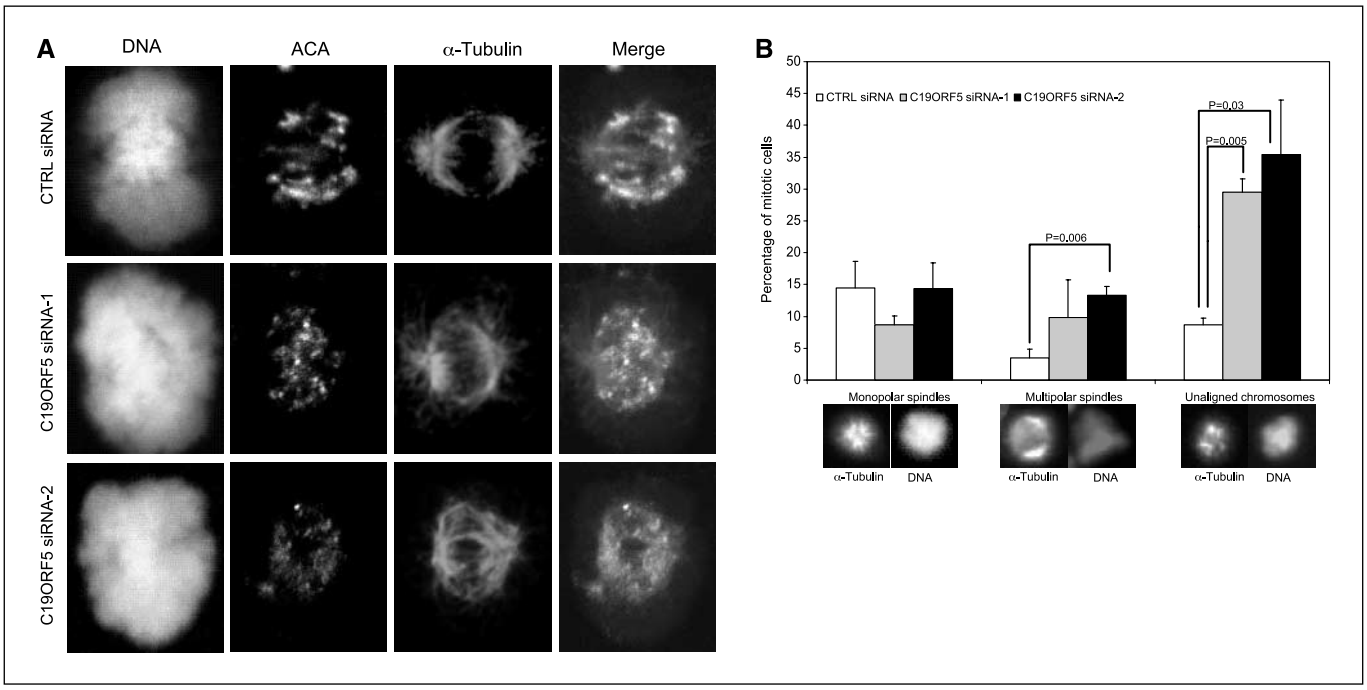

Figure 2. Spindle abnormalities caused by C19ORF5 depletion. *A,* mitotic cells were collected by shake-off 48 h posttransfection of HeLa cells with the siRNA oligos indicated, placed on poly-L-lysine–coated coverslips before extraction and methanol fixation (−20°C, 10 min). The fixed cells were then stained with antibodies against human anticentromeres (*ACA*) and α-tubulin. The DNA was counterstained with DAPI. Deconvoluted images were collected with confocal microscopy. *B,* following visualization of α-tubulin and DAPI, as described in Materials and Methods, the state of the spindle polarity as well as other abnormalities in the metaphase cells was noted (n = 150). *Bars,* SD of three experiments. The *P* values were determined using Student's *t* test.

software from Digital Scientific (Cambridge, United Kingdom). For confocal microscopy, slides were analyzed with Zeiss confocal microscope system and deconvoluted images were obtained by analysis with NIH ImageJ software.

Time-lapse video recording of mitosis. Approximately 1×10^5 cells per well of control or C19ORF5-depleted HeLa-H2B-GFP cells were seeded in a 24-well plate 24 h after transfection. The next day, time-lapse video recording was done at an interval of 2 min using a microscope (AxioVert 200,

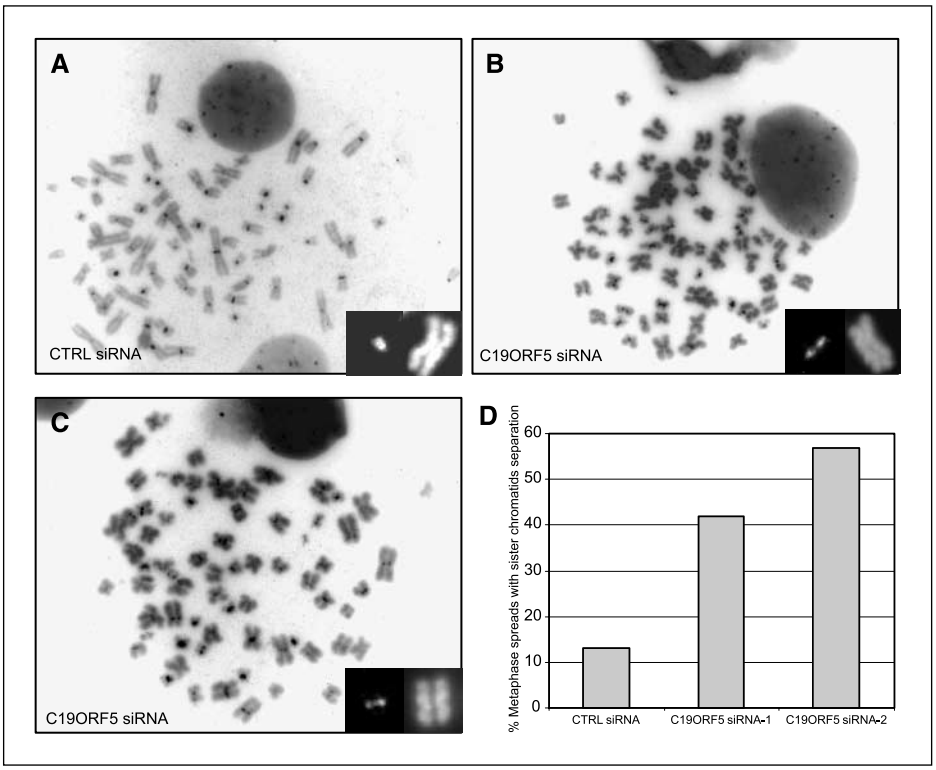

Figure 3. Analysis of chromosomes and aneuploidy following C19ORF5 depletion. *A* to *C,* inverted images of DAPI/Cy3-centromeric FISH-stained metaphase spreads. *Insets,* magnified chromosomes and their centromeres. Pan-centromeric FISH analysis shows the extent of sister chromatid separation at the centromeres. *D,* frequency of metaphase spreads with detectable sister chromatid separation. More than 100 metaphase spreads from at least three transfections were analyzed for the presence of sister chromatid separation.

Downloaded from cancerres.aacrjournals.org on January 21, 2021. © 2007 American Association for Cancer Research.

Carl Zeiss MicroImaging, Inc., Welwyn Garden City, United Kingdom) equipped with a camera and a CO_2 incubator unit. Phase-contrast and fluorescent video images were visualized using the computer software attached to the microscope system (SimplePCI).

Microtubule regrowth assay. Cells were incubated with either 330 nmol/L or 10 μmol/L nocodazole (Sigma-Aldrich; overnight or 1 h, respectively) before washout. Nocodazole was washed out thrice using PBS followed by the addition of fresh DMEM, allowing the cells to recover at 37°C, 5% CO_2 for the times indicated. Microtubule regrowth was stopped by fixing the cells with methanol and immunofluorescence was done as above.

Preparation of metaphase spreads and centromeric fluorescence *in situ* hybridization. Four days after siRNA treatment, $\sim 2 \times 10^5$ cells were treated for 1.5 to 3 h with media supplemented with colcemid at a final concentration of 100 ng/mL. Cells were harvested by trypsinization, washed with PBS, and one tenth of the cells were reserved for Western blotting. The remaining cells were processed for obtaining metaphase spreads as previously described (27). For fluorescence *in situ* hybridization (FISH), slides were dehydrated through 70%, 90%, and 100% ethanol, then hybridized with Cy3-labeled human pan-centromeric chromosome paint (CamBio, Cambridge, United Kingdom) according to the manufacturer's protocol.

Results

Mitotic abnormalities following C19ORF5 depletion. To try and understand the function(s) of endogenous C19ORF5 in mammalian cells, we used siRNA-mediated silencing in HeLa cells to deplete C19ORF5 and observe the resulting phenotype(s). We could achieve significant reduction of C19ORF5 protein levels within 48 h of transfection using two independent siRNA oligos and using an siRNA oligo directed to the Luciferase gene as a control (Fig. 1*A*). Song et al. (18) have recently shown that a HeLa clone stably expressing short hairpin RNA constructs directed against C19ORF5 progress through mitosis in an accelerated and aberrant manner. To examine the effects of transient depletion of C19ORF5 on mitosis, we used HeLa cells stably expressing GFP-tagged histone H2B and recorded the process of mitosis by time-lapse microscopy (26). We have used the point of nuclear envelope breakdown as time 0 and the onset of anaphase as the end point. This is in contrast to the timing used by Song et al. (18) wherein they took late prometaphase as time 0. We have found that the majority of control siRNA–transfected cells undergo cell division within 50 to 60 min (Fig. 1*B* and *C*). However, the majority of C19ORF5-depleted cells took 4 h or longer for a small number of cells to eventually proceed to anaphase. During that time, cells could go through the nuclear envelope breakdown and prometaphase but they were unable to form a stable metaphase plate with all the chromosomes aligned to it (Fig. 1*B*). To confirm this observation in a different assay, we have measured the mitotic index following C19ORF5 depletion in the parental HeLa cells (Fig. 1*D*). The findings indicate an inverse relationship between C19ORF5 expression and the mitotic index, which correlated with the delay in progressing through metaphase transition. DNA histograms also indicate an accumulation of cells in the G_2-M phase of the cell cycle (Fig. 1*E*). Measurement of cyclin B and cyclin A levels in those cells show a modest increase in the levels of cyclin B following C19ORF5 depletion (Fig. 1*F*). To understand the molecular mechanisms underlying this observed phenotype, we analyzed the spindle microtubules following C19ORF5 knockdown. As shown in Fig. 2*A*, the spindles look abnormal and the microtubule fibers generally lack the organization observed in control-treated cells. Although the spindles are mostly bipolar, the poles are not well defined as in control cells. Staining the centromeres and the chromatin shows lack of

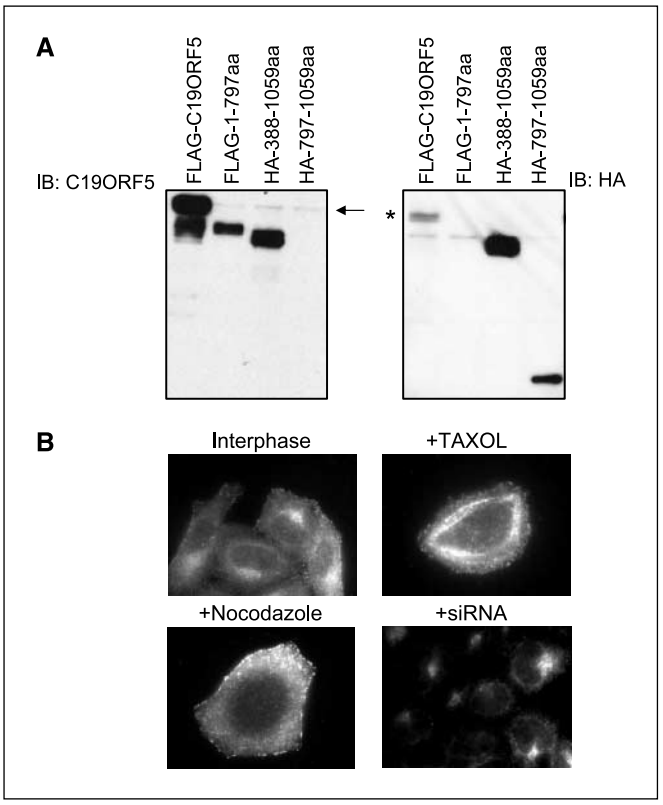

Figure 4. Validation of mAb4G1 mouse anti-C19ORF5 mAb for Western blotting and immunofluorescence. *A,* in addition to using siRNA-mediated knockdown, full-length C19ORF5 and deletions generated from C19ORF5 were used to map the antibody binding region to amino acids 388 to 797. The multiple bands detected may reflect phosphorylation or other posttranslational modifications. The faint band indicated with an arrow (*left*) is endogenous C19ORF5 in HeLa cells. The band indicated with an asterisk (*right*) is remaining signal from FLAG-C19ORF5 that stripping did not manage to remove. *B,* methanol-fixed cells treated with vehicle, 10 μmol/L paclitaxel, or 10 μmol/L nocodazole for 1 h, as well as C19ORF5 siRNA-1 transfected cells, were incubated with anti-C19ORF5 antibody for 1 h at room temperature and subsequently with antimouse Alexa Fluor 594–conjugated antibody.

condensation and compactness (Fig. 2*A*). When cells eventually proceed to anaphase and telophase, they do so erratically with a notable reduction or disorganization of the astral microtubules. We could not detect any significant changes in the fraction of monopolar spindles (Fig. 2*B*). In contrast, there was a 2-fold increase in the fraction of mitotic cells with multipolar spindles following C19ORF5 depletion (Fig. 2*B*). The largest change, however, was the large increase in the percentage of metaphase cells exhibiting metaphase plates with incomplete chromosome alignment following C19ORF5 depletion in HeLa cells (Fig. 2*B*).

C19ORF5-depleted HeLa cells were observed to have a problem in properly aligning the chromosomes to the metaphase plate, resulting in lagging chromosomes during anaphase (Figs. 1*B* and 2*B*). We therefore hypothesized that altering C19ORF5 levels may cause aneuploidy and alterations in chromosome numbers. To test this assumption, we prepared and examined metaphase spreads from control or C19ORF5-depleted HeLa cells, 96 h after transfection. The average chromosome numbers in control siRNA–treated HeLa cells were $\sim$64 with a median of 68 and a mode of 71. However, the average chromosome number in C19ORF5-depleted cells was 66 with a median of 68 and a mode of 72. In addition, preliminary M-Fish analysis of the metaphase spreads confirms

Downloaded from cancerres.aacrjournals.org on January 21, 2021. © 2007 American Association for Cancer Research.

that there is an elevated alteration in chromosomal numbers after C19ORF5 depletion. The most frequent change, however, was the increase in the incidence of sister chromatid separation (Fig. 3). In control-treated HeLa cells, chromosome arms were well resolved but the centromeres were closely associated as would be expected of normal centromeric cohesion. In contrast, chromosomes in C19ORF5-depleted HeLa cells frequently appeared as individual chromatids (Fig. 3). To confirm that these were indeed individual sister chromatids, we did pan-centromeric FISH analysis. The centromeric signals were as expected in control spreads (i.e., two closely attached chromatids). However, the centromeres from the C19ORF5-depleted cell spreads were often separated, which confirms that depletion of C19ORF5 is associated with premature separation of sister chromatids and loss of centromeric cohesion (Fig. 3).

C19ORF5 decorates the spindle microtubules. Because C19ORF5 seems to only decorate stable microtubules and its knockdown causes spindle abnormalities, we reasoned that

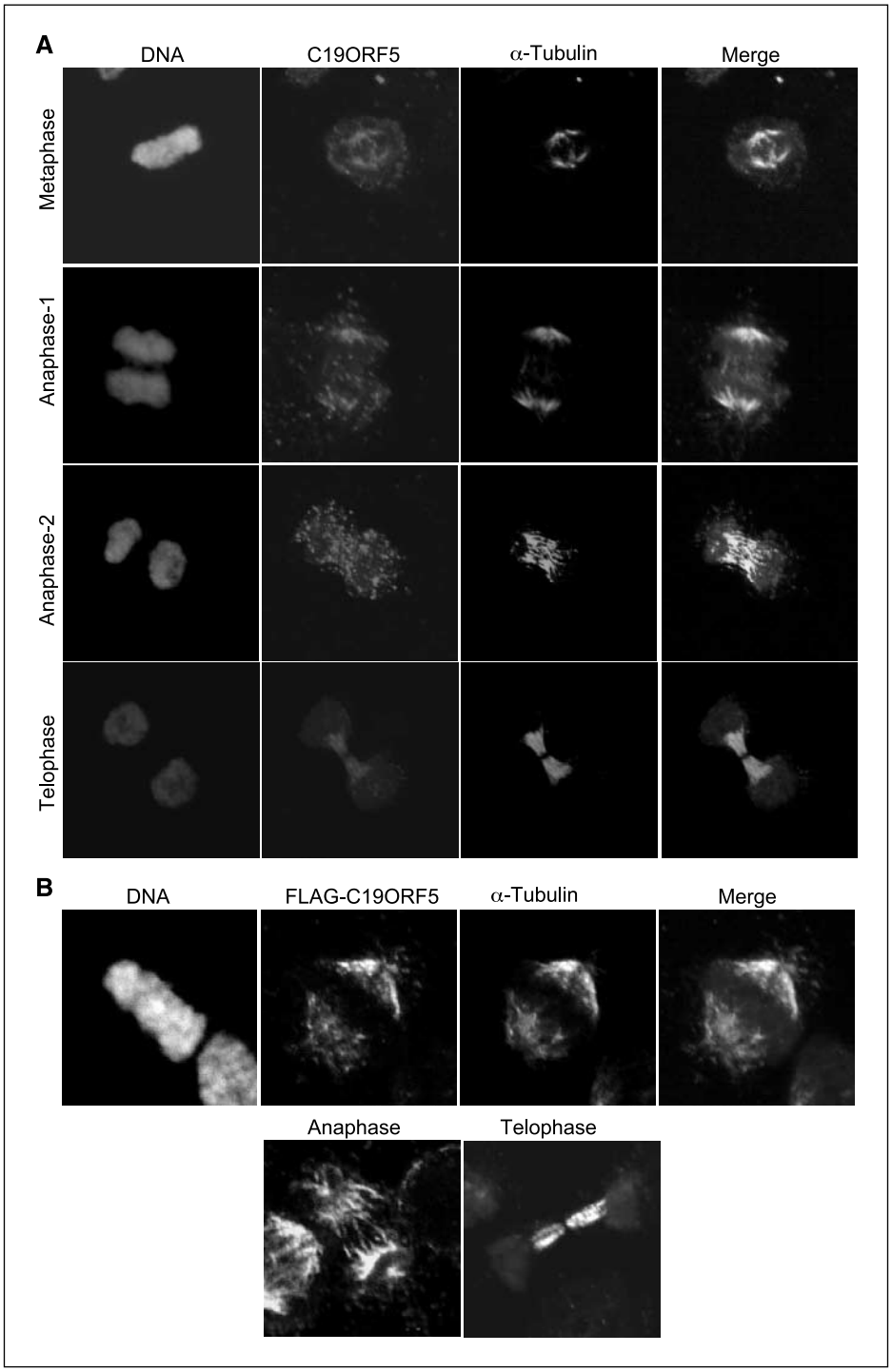

Figure 5. Mitotic HeLa cells were collected by shake-off and placed on poly-L-lysine–coated coverslips before extraction with 0.2% Triton X-100 in PHEM buffer and methanol fixation (−20°C, 10 min). The fixed cells were stained with mouse anti-C19ORF5 mAb or rabbit polyclonal anti–α-tubulin antibody. The DNA was counterstained with DAPI. Deconvoluted images were obtained by confocal microscopy. *B*, HeLa cells expressing FLAG-C19ORF5 for 16 h posttransfection were collected and fixed as in (*A*) before incubation with mouse anti-FLAG antibody and rabbit polyclonal anti–α-tubulin antibody. Full color figures are available on request.

Downloaded from cancerres.aacrjournals.org on January 21, 2021. © 2007 American Association for Cancer Research.

C19ORF5 microtubule association is dynamic and requires undetermined modification of the microtubules. Therefore, we used the mAB4G1 antibody to study the localization of endogenous C19ORF5 throughout the cell cycle. First, we further validated the specificity of the antibody and mapped it to the region amino acids 388 to 797 of C19ORF5 (Fig. 4*A*). This is in agreement with Liu et al. (25). We have used the same antibody in immunofluorescence analysis and found that the best signal is given following methanol fixation. In interphase cells, endogenous C19ORF5 shows, similar to the overexpressed protein, a diffuse cytoplasmic staining with partial localization to the microtubules (Fig. 4*B*). The microtubule localization of the endogenous protein was confirmed by its disruption when treated with either nocodazole or paclitaxel (Fig. 4*B*). Mitotic cells, however, showed stronger staining for C19ORF5 and the protein can be clearly seen at the spindle microtubules during the different stages of mitosis (Fig. 5*A*). As a control, we also transfected FLAG-C19ORF5 and stained the mitotic cells with anti-FLAG antibody. As shown in Fig. 5*B*, FLAG-C19ORF5 also localizes to the spindle microtubules throughout mitosis (Fig. 5*B*). We have also determined that only the full-length C19ORF5 can localize to the spindle because deleting either the NH_2 terminus or COOH terminus disrupted this localization (data not shown).

C19ORF5 expression is required for anchoring the microtubules to the centrosome. C19ORF5 is a microtubule-associated protein that is unusual in its inability to protect the microtubules against nocodazole-induced depolymerization. To further elucidate the role of C19ORF5 in the microtubule organization, we treated control or C19ORF5-depleted HeLa-H2B-GFP cells with 330 nmol/L nocodazole for 16 h to block the majority of cells at prometaphase before washout and video recorded mitosis by time-lapse microscopy (Fig. 6; Supplementary movies). This treatment with nocodazole completely depolymerizes the microtubules as shown in Fig. 8*B*. Whereas the control-transfected cells recovered and proceeded to anaphase within 50 min of nocodazole washout, the majority of C19ORF5-depleted cells took significantly longer time to divide after nocodazole washout (Fig. 6). This indicated that C19ORF5 depletion may have caused a delay in microtubule repolymerization or it may have caused other related defects. To test this, we did the microtubule regrowth assay following C19ORF5 knockdown and stained the mitotic cells with antibodies against C19ORF5 and α-tubulin/γ-tubulin or pericentrin (Fig. 7). At time 0 after nocodazole washout, there was complete depolymerization of the microtubules and C19ORF5 was detected as diffused cytosolic staining (data not shown). Following recovery for 10 min, in control-treated cells, the microtubule-organizing centers, stained with α-tubulin/γ-tubulin antibodies, appear as expected at the spindle poles, which colocalize with endogenous C19ORF5 that appears as a concentrated signal at the microtubule-organizing center. In contrast, there was a considerable lack of a recognizable microtubule-organizing center in the C19ORF5-depleted cells, as indicated by a lack of C19ORF5 expression, where α-tubulin seems to be radiating from multiple sites and not from the spindle poles (Fig. 7*A*). As well as in mitotic cells, interphase cells treated in a similar fashion exhibited similar phenotypes (data not shown). Song et al. (18) reported that C19ORF5 depletion causes centrosome fragmentation as shown by γ-tubulin staining. We could detect similar levels of γ-tubulin fragmentation in interphase cells (data not shown). In addition, following recovery from nocodazole, fibers of γ-tubulin can be seen enveloping the chromatin instead of the spindle poles; fragments of random sizes of γ-tubulin can also be seen where C19ORF5 is depleted. To test whether C19ORF5 depletion disrupts the anchoring and organization of the centrosomes or exerts its effects through anchoring of γ-tubulin and microtubule nucleation, we stained the C19ORF5-depleted cells with antibodies against pericentrin and C19ORF5. Surprisingly, C19ORF5 depletion did not affect pericentrin localization either in untreated cells or following nocodazole washout (Fig. 7*D*). This may indicate that the centrosomal abnormalities seen following C19ORF5 depletion reflect γ-tubulin fragmentation and lack of stable anchoring to the centrioles.

The NH_2 terminus of C19ORF5 is required for microtubules anchoring. To establish which part of C19ORF5 protein is required

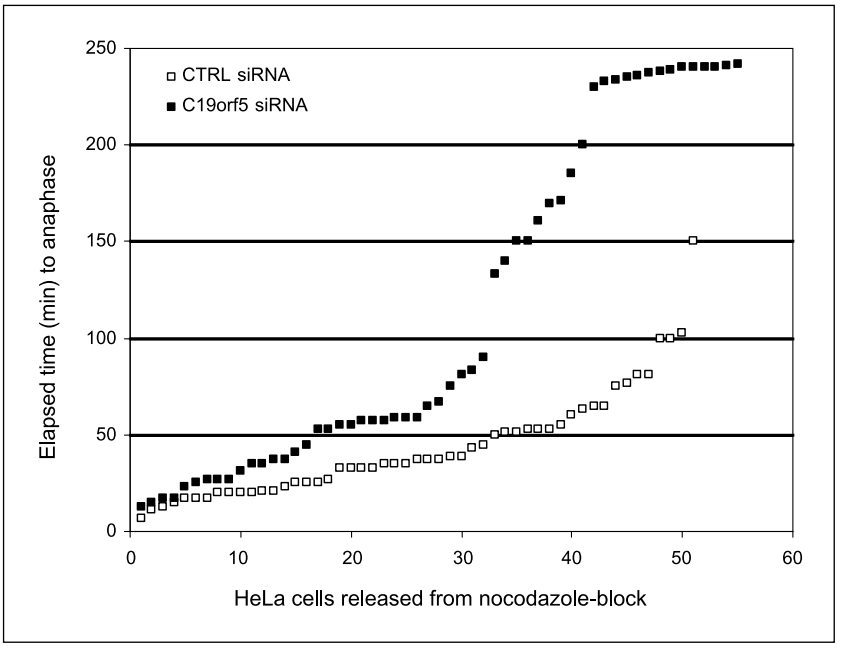

Figure 6. C19ORF5 depletion delays microtubule polymerization. HeLa-H2B-GFP cells were treated with either control siRNA or C19ORF5 siRNA-2 for 48 h before addition of 330 nmol/L nocodazole and overnight incubation. Cells blocked at prometaphase were collected by shake-off and washed thrice with PBS before resuspension in normal growth medium and the start of time-lapse video microscopy for 4 h. The cells were ordered ascending according to the elapsed time to anaphase.

Downloaded from cancerres.aacrjournals.org on January 21, 2021. © 2007 American Association for Cancer Research.

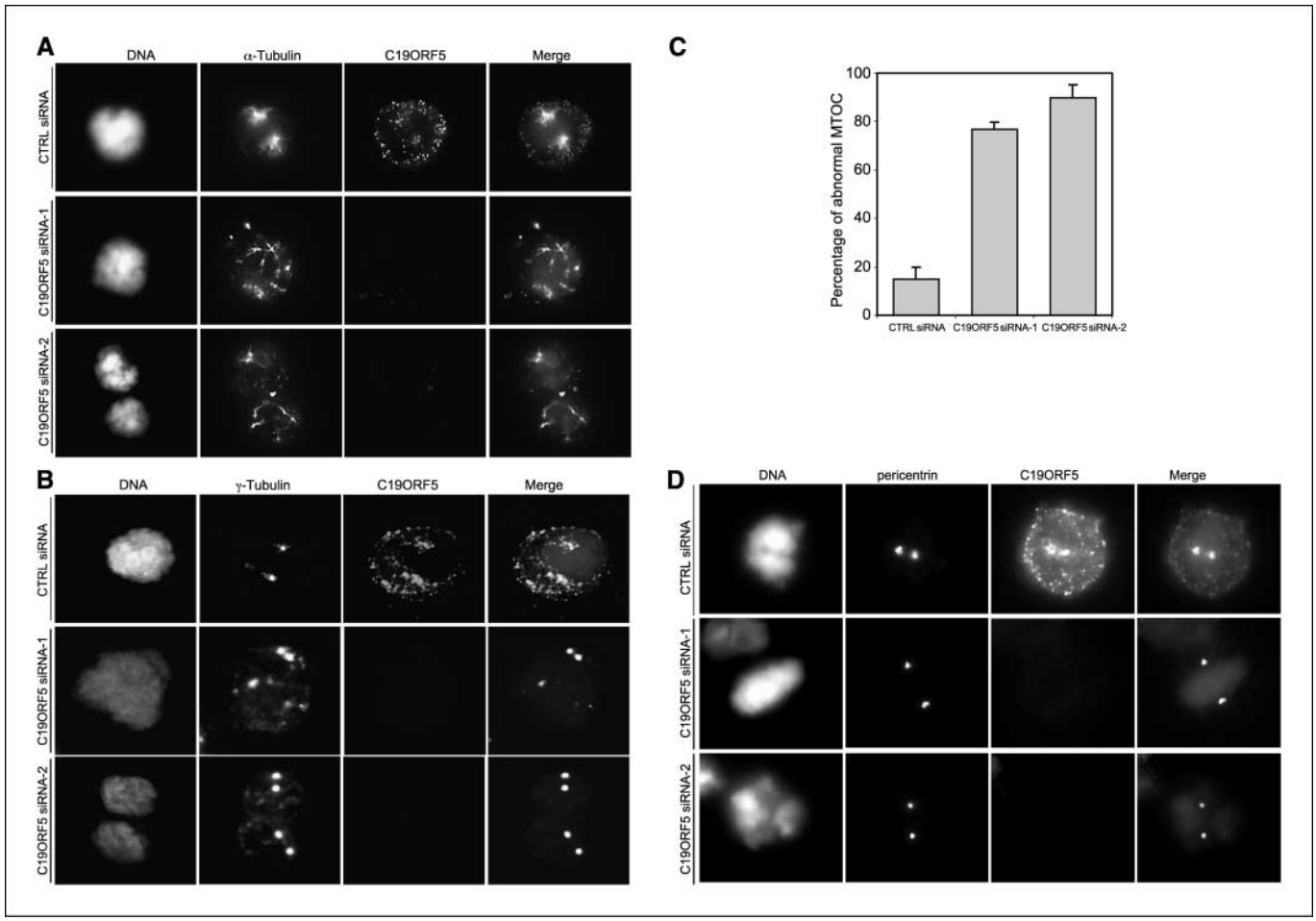

Figure 7. C19ORF5 is required for anchoring of the microtubule-organizing center. *A,* microtubule nucleation assay was done on HeLa cells wherein cells treated with the different oligos were incubated in nocodazole before washout and recovery for 10 min in normal growth medium. Fixed cells were stained for C19ORF5 and α-tubulin/γ-tubulin (*A* and *B*) or pericentrin (*D*) to visualize the microtubule-organizing center (*MTOC*) and the centrosomes. *C,* quantification of the fraction of mitotic cells exhibiting abnormal microtubule nucleation ($n = 100$). Cells were blocked in prometaphase by incubation with nocodazole overnight before mitotic shake-off and placing on poly-L-lysine–coated coverslips. The microtubules were allowed to recover for 10 min before fixation with methanol and incubation with anti–α-tubulin/γ-tubulin antibodies and counting. *Bars,* SD of three experiments.

for localizing to the microtubule-organizing center following nocodazole washout, we transfected HeLa cells with full-length FLAG-C19ORF5, FLAG-C19ORF5-1-797aa, HA-C19ORF5-388-1059aa, or HA-C19ORF5-797-1059aa (Fig. 8*A*) and did the microtubule nucleation assay as above but staining the cells with either FLAG-HA and γ-tubulin antibodies (Figs. 8 and 4*A* for expression levels). As shown in Fig. 8*C*, only the full-length C19ORF5 and amino acid 1 to 797 constructs localized to the microtubule-organizing center whereas the other two constructs did not. The amino acid 1 to 797 deletion lacks the COOH-terminal putative light chain whereas the amino acid 388 to 1,059 construct has a truncated putative heavy chain (Fig. 8*A*). This shows that the NH_2 terminus putative heavy chain is required for microtubule-organizing center localization and is potentially important for anchoring the microtubule-organizing center.

Discussion

There is an ever increasing amount of evidence for considering RASSF1A as a bona fide tumor suppressor gene (1). It remains, however, difficult to ascertain how RASSF1A can exert its tumor suppressive functions. Understanding the functions of the RASSF1A-interacting microtubule-associated protein C19ORF5 will yield greater understanding of the RASSF1A-regulated signaling pathways and ultimately will benefit our understanding of the multiple steps of carcinogenesis. Song et al. (18) suggested that C19ORF5 (or RABP1 as they refer to it in their article) is a centrosomal protein responsible for recruiting RASSF1A to the spindle poles where it can exert inhibitory actions on the activation of the anaphase-promoting complex/Cdc20 complex and block the prometaphase to metaphase progression. The authors have also reported that depletion of C19ORF5/RABP1 accelerates mitotic progression and increases the frequency of abnormal mitosis. We extended on these observations, but instead of using short hairpin RNA–mediated stable knockdown, we have opted for the transient treatment with siRNA oligos. Using two independent siRNA oligos directed against C19ORF5 and a control oligo directed against the luciferase gene, we show that C19ORF5 depletion in HeLa cells actually delays mitosis. The C19ORF5-depleted cells are able to form the metaphase plate but that happens transiently and in an unstable fashion. The end result is an increase in the mitotic index and the frequency of

Downloaded from cancerres.aacrjournals.org on January 21, 2021. © 2007 American Association for Cancer Research.

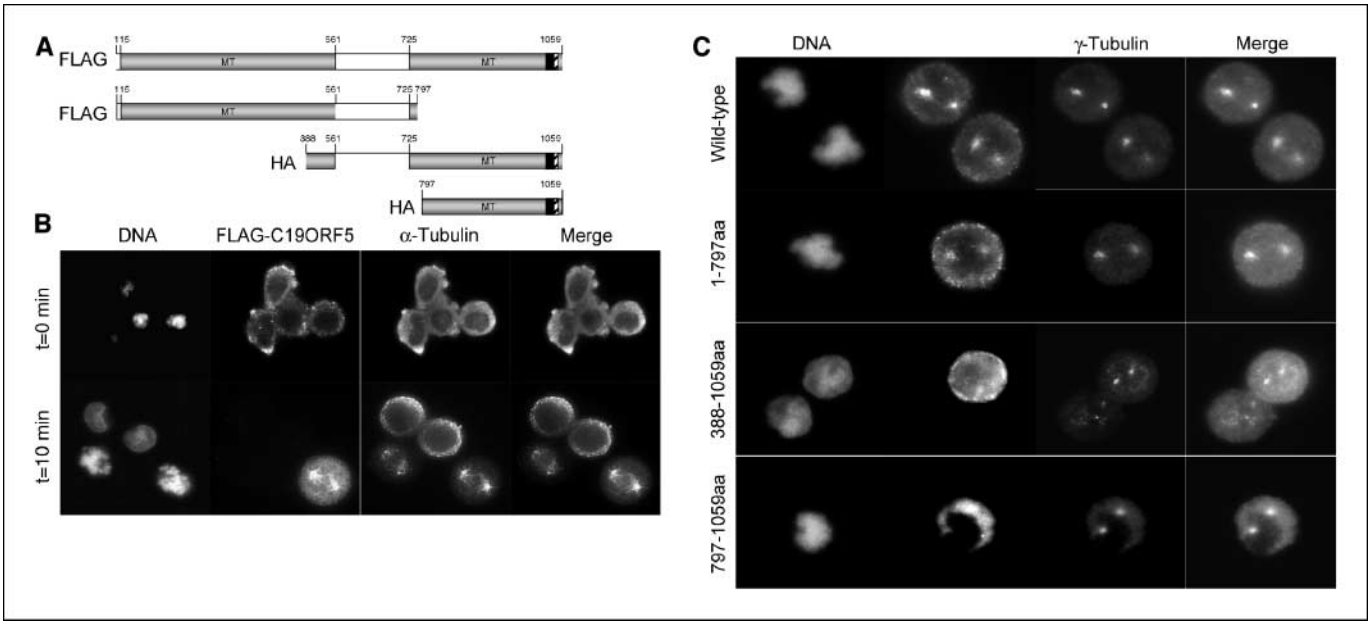

Figure 8. The NH_2 terminus of C19ORF5 is required for localization to the microtubule-organizing center during nucleation. *A,* schematic diagram representing the deletion constructs used. *Black shaded area,* an essential microtubule-association area as determined by Liu et al. (20); *dashed area,* mitochondria accumulation and genome destruction (*MAGD*) as also determined by Liu et al. (20). *Gray shades,* areas of homology to MAP1A and MAP1B microtubule-associated regions. *B,* the localization of FLAG-C19ORF5 at time 0 and *t* = 10 min after nocodazole washout. Note the complete depolymerization of the microtubules. *C,* only the full-length C19ORF5 and amino acid 1 to 797 constructs localized to the microtubule-organizing center after nocodazole washout.

metaphase cells with unaligned chromosomes. The spindle is also activated because we could detect BUBR1 at the kinetochores of C19ORF5-depleted cells (data not shown). The discrepancy between these findings and the findings reported by Song et al. (18) maybe attributed to differences between transient and stable depletion of C19ORF5. In addition, we have timed mitosis from the point of nuclear envelope breakdown to the onset of anaphase, instead of late prometaphase to anaphase as previously reported (18).

In this study, we show that C19ORF5 localization is not restricted to the centrosomes and it does decorate the spindle microtubules during mitosis. We have attempted a variety of fixation methods and cell lines, but we consistently observed that the majority of either endogenous or exogenous C19ORF5 localized to the spindle with some present in the cytosol. Additionally, we could detect C19ORF5 concentrating at the microtubule-organizing center during microtubule regrowth. We cannot exclude the possibility of centrosomal localization because the antibody used in ref. 18 maps to different regions of C19ORF5, which, as a result of potential proteolytic cleavage, may concentrate at the centrosomes. Due to the predicted multiple layers of posttranslational modifications exerted on C19ORF5, we cannot exclude the possibility that an undetectable fraction of the protein may reside at the kinetochores functioning in microtubule-kinetochores attachments.

Based on C19ORF5 localization and ability to bind to the microtubules (20, 23), we hypothesized that the mitotic problems associated with C19ORF5 depletion result from aberrant microtubule dynamics. We have found that the spindle is abnormal throughout mitosis in C19ORF5-depleted cells. In addition, we have completely depolymerized the microtubules in HeLa-H2B-GFP cells, which caused the cells to be blocked at prometaphase. The prolonged time that the C19ORF5-depleted cells took to proceed to anaphase following nocodazole washout strongly indicated that these cells are slower in repolymerizing the microtubules and forming the spindle. We do not have evidence for a slower microtubule repolymerization caused by C19ORF5 depletion. Instead, we have identified a novel role for C19ORF5 in anchoring α- and γ-tubulin to the centrosomes during microtubule nucleation and regrowth. C19ORF5, whether endogenous or overexpressed, concentrates at the microtubule-organizing centers within 1 min following nocodazole recovery (data not shown). When C19ORF5 is depleted in mitotic cells, the microtubules appear to be nucleated from multiple sites. C19ORF5 depletion does not seem to affect the centriole position at the centrosome because pericentrin does not seem to be affected, although γ-tubulin appear fragmented, giving the impression of a fragmented or duplicated centrosome.

The mechanism by which the sister chromatids separate prematurely when C19ORF5 is depleted is unknown. It could be argued that, based on Song et al. (18), C19ORF5 depletion could perturb the intricate regulation of the anaphase-promoting complex activity and therefore cause the premature degradation of securin. An alternative mechanism is that altered spindle dynamics causes changes to the spindle pulling and pushing forces on the kinetochores, thus perhaps affecting chromatids cohesion at the centromeres. It has recently been shown that depletion of the microtubule-associated proteins, anaphase-promoting complex, and EB1 increases the frequency of chromosome misalignment and lagging (28).

We have shown in this study that expression of C19ORF5 is required for mitotic fidelity, functioning as an anchoring protein for γ-tubulin and the microtubule-organizing center in mitotic cells. This adds to its function as a docking agent for RASSF1A to the centrosome. Considering the emerging active role microtubules play in apoptosis (29), as well as their established role in the spindle

Downloaded from cancerres.aacrjournals.org on January 21, 2021. © 2007 American Association for Cancer Research.

formation during mitosis, the RASSF1A-C19ORF5 interaction is an intriguing link between the microtubules, cell cycle control, and apoptosis. The disruption of this pathway, as evident in several types of human cancers, may have a large effect on the process of tumorigenesis. In fact, truncating mutations in C19ORF5 have recently been identified in colorectal tumor cell lines (30). Incidentally, colorectal cancers exhibit a relatively low percentage of RASSF1A methylation inactivation (1).

Acknowledgments

Received 9/28/2006; revised 11/15/2006; accepted 11/22/2006.

Grant support: Association for International Cancer Research, Sport Aiding Medical Research for Kids, Cancer Research UK, Breast Cancer Campaign, and Birmingham Children's Hospital Research Foundation (F. Latif).

The costs of publication of this article were defrayed in part by the payment of page charges. This article must therefore be hereby marked *advertisement* in accordance with 18 U.S.C. Section 1734 solely to indicate this fact.

We thank Dr. G. Parsonage for help with time-lapse microscopy.

References

1. Agathanggelou A, Cooper WN, Latif F. Role of the Ras-association domain family 1 tumor suppressor gene in human cancers. Cancer Res 2005;65:3497–508.
2. Agathanggelou A, Honorio S, Macartney DP, et al. Methylation associated inactivation of RASSF1A from region 3p21.3 in lung, breast and ovarian tumours. Oncogene 2001;20:1509–18.
3. Dammann R, Li C, Yoon JH, Chin PL, Bates S, Pfeifer GP. Epigenetic inactivation of a RAS association domain family protein from the lung tumour suppressor locus 3p21.3. Nat Genet 2000;25:315–9.
4. Tommasi S, Dammann R, Zhang Z, et al. Tumor susceptibility of Rassf1a knockout mice. Cancer Res 2005;65:92–8.
5. van der WL, Tachibana KK, Gonzalez MA, et al. The RASSF1A isoform of RASSF1 promotes microtubule stability and suppresses tumorigenesis. Mol Cell Biol 2005;25:8356–67.
6. Song MS, Song SJ, Ayad NG, et al. The tumour suppressor RASSF1A regulates mitosis by inhibiting the APC-Cdc20 complex. Nat Cell Biol 2004;6:129–37.
7. Fenton SL, Dallol A, Agathanggelou A, et al. Identification of the E1A-regulated transcription factor p120 E4F as an interacting partner of the RASSF1A candidate tumor suppressor gene. Cancer Res 2004;64:102–7.
8. Shivakumar L, Minna J, Sakamaki T, Pestell R, White MA. The RASSF1A tumor suppressor blocks cell cycle progression and inhibits cyclin D1 accumulation. Mol Cell Biol 2002;22:4309–18.
9. Oh HJ, Lee KK, Song SJ, et al. Role of the tumor suppressor RASSF1A in Mst1-mediated apoptosis. Cancer Res 2006;66:2562–9.
10. Rabizadeh S, Xavier RJ, Ishiguro K, et al. The scaffold protein CNK1 interacts with the tumor suppressor RASSF1A and augments RASSF1A-induced cell death. J Biol Chem 2004;279:29247–54.
11. Baksh S, Tommasi S, Fenton S, et al. The tumor suppressor RASSF1A and MAP-1 link death receptor signaling to Bax conformational change and cell death. Mol Cell 2005;18:637–50.
12. Vos MD, Dallol A, Eckfeld K, et al. The RASSF1A tumor suppressor activates Bax via MOAP-1. J Biol Chem 2006;281:4557–63.
13. Dallol A, Agathanggelou A, Tommasi S, Pfeifer GP, Maher ER, Latif F. Involvement of the RASSF1A tumor suppressor gene in controlling cell migration. Cancer Res 2005;65:7653–9.
14. Dallol A, Agathanggelou A, Fenton SL, et al. RASSF1A interacts with microtubule-associated proteins and modulates microtubule dynamics. Cancer Res 2004;64:4112–6.
15. Liu L, Tommasi S, Lee DH, Dammann R, Pfeifer GP. Control of microtubule stability by the RASSF1A tumor suppressor. Oncogene 2003;22:8125–36.
16. Vos MD, Martinez A, Elam C, et al. A role for the RASSF1A tumor suppressor in the regulation of tubulin polymerization and genomic stability. Cancer Res 2004;64:4244–50.
17. Liu L, Amy V, Liu G, McKeehan WL. Novel complex integrating mitochondria and the microtubular cytoskeleton with chromosome remodeling and tumor suppressor RASSF1 deduced by *in silico* homology analysis, interaction cloning in yeast, and colocalization in cultured cells. In Vitro Cell Dev Biol Anim 2002;38:582–94.
18. Song MS, Chang JS, Song SJ, Yang TH, Lee H, Lim DS. The centrosomal protein RAS association domain family protein 1A (RASSF1A)-binding protein 1 regulates mitotic progression by recruiting RASSF1A to spindle poles. J Biol Chem 2005;280:3920–7.
19. Orban-Nemeth Z, Simader H, Badurek S, Trancikova A, Propst F. Microtubule-associated protein 1S, a short and ubiquitously expressed member of the microtubule-associated protein 1 family. J Biol Chem 2005;280:2257–65.
20. Liu L, Vo A, Liu G, McKeehan WL. Distinct structural domains within C19ORF5 support association with stabilized microtubules and mitochondrial aggregation and genome destruction. Cancer Res 2005;65:4191–201.
21. Ding J, Allen E, Wang W, et al. Gene targeting of GAN in mouse causes a toxic accumulation of microtubule-associated protein 8 and impaired retrograde axonal transport. Hum Mol Genet 2006;15:1451–63.
22. Liu L, Vo A, Liu G, McKeehan WL. Putative tumor suppressor RASSF1 interactive protein and cell death inducer C19ORF5 is a DNA binding protein. Biochem Biophys Res Commun 2005;332:670–6.
23. Ding J, Valle A, Allen E, et al. Microtubule-associated protein 8 contains two microtubule binding sites. Biochem Biophys Res Commun 2006;339:172–9.
24. Wong EY, Tse JY, Yao KM, Lui VC, Tam PC, Yeung WS. Identification and characterization of human VCY2-interacting protein: VCY2IP-1, a microtubule-associated protein-like protein. Biol Reprod 2004;70:775–84.
25. Liu L, Vo A, McKeehan WL. Specificity of the methylation-suppressed A isoform of candidate tumor suppressor RASSF1 for microtubule hyperstabilization is determined by cell death inducer C19ORF5. Cancer Res 2005;65:1830–8.
26. Kanda T, Sullivan KF, Wahl GM. Histone-GFP fusion protein enables sensitive analysis of chromosome dynamics in living mammalian cells. Curr Biol 1998;8:377–85.
27. Trask BJ. DNA sequence localization in metaphase and interphase cells by fluorescence *in situ* hybridization. Methods Cell Biol 1991;35:3–35.
28. Draviam VM, Shapiro I, Aldridge B, Sorger PK. Misorientation and reduced stretching of aligned sister kinetochores promote chromosome missegregation in EB1- or APC-depleted cells. EMBO J 2006;25:2814–27.
29. Moss DK, Betin VM, Malesinski SD, Lane JD. A novel role for microtubules in apoptotic chromatin dynamics and cellular fragmentation. J Cell Sci 2006;119:2362–74.
30. Ivanov I, Lo KC, Hawthorn L, Cowell JK, Ionov Y. Identifying candidate colon cancer tumor suppressor genes using inhibition of nonsense-mediated mRNA decay in colon cancer cells. Oncogene. Epub 2006 Nov 6.

Downloaded from cancerres.aacrjournals.org on January 21, 2021. © 2007 American Association for Cancer Research.

AACR American Association for Cancer Research

Cancer Research
The Journal of Cancer Research (1916–1930) | The American Journal of Cancer (1931–1940)

Depletion of the Ras Association Domain Family 1, Isoform A–Associated Novel Microtubule-Associated Protein, C19ORF5/MAP1S, Causes Mitotic Abnormalities

Ashraf Dallol, Wendy N. Cooper, Fahd Al-Mulla, et al.

Cancer Res 2007;67:492-500.

Updated version	Access the most recent version of this article at: http://cancerres.aacrjournals.org/content/67/2/492
Supplementary Material	Access the most recent supplemental material at: http://cancerres.aacrjournals.org/content/suppl/2007/01/15/67.2.492.DC1

Cited articles	This article cites 29 articles, 17 of which you can access for free at: http://cancerres.aacrjournals.org/content/67/2/492.full#ref-list-1
Citing articles	This article has been cited by 13 HighWire-hosted articles. Access the articles at: http://cancerres.aacrjournals.org/content/67/2/492.full#related-urls

E-mail alerts	Sign up to receive free email-alerts related to this article or journal.
Reprints and Subscriptions	To order reprints of this article or to subscribe to the journal, contact the AACR Publications Department at pubs@aacr.org.
Permissions	To request permission to re-use all or part of this article, use this link http://cancerres.aacrjournals.org/content/67/2/492. Click on "Request Permissions" which will take you to the Copyright Clearance Center's (CCC) Rightslink site.

Downloaded from cancerres.aacrjournals.org on January 21, 2021. © 2007 American Association for Cancer Research.